



PERGAMON

Available online at www.sciencedirect.com

SCIENCE @ DIRECT®

Polyhedron 22 (2003) 3009–3014



POLYHEDRON

www.elsevier.com/locate/poly

# Hydrogen-bonding as a tool for building one-dimensional structures based on dimetal building blocks

Jitendra K. Bera <sup>a</sup>, Thanh-Trang Vo <sup>a</sup>, Richard A. Walton <sup>b</sup>, Kim R. Dunbar <sup>a,\*</sup>

<sup>a</sup> Department of Chemistry, Texas A&M University, P.O. Box 30012, College Station, TX 77842-3012, USA

<sup>b</sup> Department of Chemistry, Purdue University, 1393 Brown Building, West Lafayette, IN 47907-1393, USA

Received 20 May 2002; accepted 28 July 2002

## Abstract

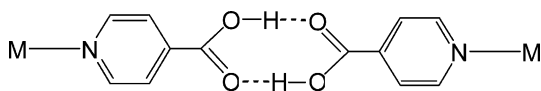
The ligands isonicotinamide and nicotinamide are used to form assemblies of dimetal ( $M_2$ ) building units via a combination of coordinate bonds and intermolecular hydrogen-bond interactions. Polymeric networks of the linear, zig-zag and sinusoidal varieties are observed in the solid state depending on the ligands and metal precursors involved.

© 2003 Elsevier Ltd. All rights reserved.

**Keywords:** Ligands; Molecular assemblies; Metal precursors; Polymeric network

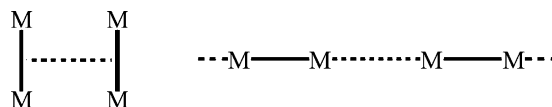
## 1. Introduction

A perusal of the literature reveals a large number of compounds based on the use of polydentate ligands to join metal units into infinite structures [1]. One strategy for preparing extended structures with metal building blocks is to use supramolecular interactions such as hydrogen bonds and  $\pi$ - $\pi$  interactions as tools to prepare materials with predictable structures [2]. In this vein, pyridine carboxylic acids and carboxyamides have been used with a variety of metal ions to form hydrogen-bonded frameworks based on the linking unit depicted below [3].



In recent years, the use of dimetal ( $M_2$ ) precursors in the construction of molecular assemblies has become a subject of active research [4]. Two limiting cases of

joining  $M_2$  units, namely the perpendicular (equatorial bridges) and parallel (axial bridges) orientations, can be accomplished by specific choices of bridging ligands. Suitable equatorial and axial linkers are dicarboxylate and polypyridine ligands, respectively. The strong tendency of  $Rh_2(O_2CR)_4$  complexes to form axial interactions has led to the isolation of a large number of extended arrays based on these molecules whose dimensions and topologies are dictated by the arrangement of the donor sites on the ligands [5]. Recent work performed in our laboratories points to analogous chemistry for the quadruply bonded dirhenium complex  $cis-Re_2(O_2CCH_3)_2Cl_4 \cdot (H_2O)_2$ . For example, reactions of  $Re_2(O_2CCH_3)_2Cl_4 \cdot (H_2O)_2$  with pyrazine (pyz) and 4,4'-bipyridine (4,4'-bpy) lead to the formation of one-dimensional (1-D) polymers of general formula  $[Re_2(O_2CCH_3)_2Cl_4(LL)_2]_n$  ( $LL = \text{pyz}, 4,4'\text{-bpy}$ ) [6].



As a continuation of our interest in the application of supramolecular chemistry to the preparation of new structures based on dimetal complexes, we now report the use of pyridine carboxyamides as axial ligands for

\* Corresponding author. Fax: +1-979-845-7177.

E-mail address: [dunbar@mail.chem.tamu.edu](mailto:dunbar@mail.chem.tamu.edu) (K.R. Dunbar).

dirhodium and dirhenium compounds. In addition to acting as pyridine donors to the axial sites, the ligands engage in intermolecular hydrogen bonding to form polymeric networks of the linear, zig-zag and sinusoidal varieties.

## 2. Experimental

### 2.1. Materials and synthesis

The ligands nicotinamide (NIA) and isonicotinamide (INA) were purchased from Aldrich and used as received. The starting materials *cis*-Re<sub>2</sub>(O<sub>2</sub>CCH<sub>3</sub>)<sub>2</sub>Cl<sub>4</sub>(H<sub>2</sub>O)<sub>2</sub> [7] and Rh<sub>2</sub>(O<sub>2</sub>CCH<sub>3</sub>)<sub>4</sub> [8] were prepared as described in the literature. All other reagents and organic solvents were purchased from commercial sources. Elemental microanalyses were performed by Dr. H.D. Lee of the Purdue University Microanalytical Laboratory.

### 2.2. Synthesis of Rh<sub>2</sub>(O<sub>2</sub>CCH<sub>3</sub>)<sub>4</sub>(INA)<sub>2</sub>·2(CH<sub>3</sub>)<sub>2</sub>CO (1)·2(CH<sub>3</sub>)<sub>2</sub>CO

A saturated acetone solution of isonicotinamide was carefully layered on an acetone solution (10 ml) of Rh<sub>2</sub>(O<sub>2</sub>CCH<sub>3</sub>)<sub>4</sub> (0.015 g, 0.03 mmol) in an 8 mm Pyrex tube. After 2 days, purple crystals of **1** were collected and washed with acetone and dried in air. *Anal.* Calc.

for C<sub>26</sub>H<sub>36</sub>N<sub>4</sub>O<sub>12</sub>Rh<sub>2</sub>: C, 38.92; H, 4.52; N, 6.98. Found: C, 39.03; H, 4.57; N, 6.88%.

### 2.3. Synthesis of Rh<sub>2</sub>(O<sub>2</sub>CCH<sub>3</sub>)<sub>4</sub>(NIA)<sub>2</sub>·2(CH<sub>3</sub>)<sub>2</sub>CO (2)·2(CH<sub>3</sub>)<sub>2</sub>CO

A procedure similar to the one described in Section 2.2 was used to prepare **2** from Rh<sub>2</sub>(O<sub>2</sub>CCH<sub>3</sub>)<sub>4</sub> and nicotinamide. *Anal.* Calc. for C<sub>26</sub>H<sub>36</sub>N<sub>4</sub>O<sub>12</sub>Rh<sub>2</sub>: C, 38.92; H, 4.52; N, 6.98. Found: C, 38.72; H, 4.47; N, 6.91%.

### 2.4. Synthesis of *cis*-Re<sub>2</sub>(O<sub>2</sub>CCH<sub>3</sub>)<sub>2</sub>Cl<sub>4</sub>(INA)<sub>2</sub> (3)

A procedure similar to the one described in Section 2.2 was used to prepare **3** from *cis*-Re<sub>2</sub>(O<sub>2</sub>CCH<sub>3</sub>)<sub>2</sub>Cl<sub>4</sub>(H<sub>2</sub>O)<sub>2</sub> (0.020 g, 0.03 mmol) and nicotinamide to yield green crystals of **3**. *Anal.* Calc. for C<sub>16</sub>H<sub>18</sub>Cl<sub>4</sub>N<sub>4</sub>O<sub>6</sub>Re<sub>2</sub>: C, 21.92; H, 2.07; N, 6.39. Found: C, 21.86; H, 2.02; N, 6.21%.

### 2.5. Synthesis of *cis*-Re<sub>2</sub>(O<sub>2</sub>CCH<sub>3</sub>)<sub>2</sub>Cl<sub>4</sub>(NIA)<sub>2</sub>·2(NIA) (4)·2(NIA)

A procedure similar to the one described in Section 2.4 was used to prepare **4** from *cis*-Re<sub>2</sub>(O<sub>2</sub>CCH<sub>3</sub>)<sub>2</sub>Cl<sub>4</sub>(H<sub>2</sub>O)<sub>2</sub> and nicotinamide. *Anal.* Calc. for C<sub>28</sub>H<sub>30</sub>Cl<sub>4</sub>N<sub>8</sub>O<sub>8</sub>Re<sub>2</sub>: C, 30.01; H, 2.70; N, 10.00. Found: C, 29.83; H, 2.62; N, 9.62%.

Table 1

Crystallographic data for Rh<sub>2</sub>(O<sub>2</sub>CCH<sub>3</sub>)<sub>4</sub>(INA)<sub>2</sub>·2(CH<sub>3</sub>)<sub>2</sub>CO (**1**)·2(CH<sub>3</sub>)<sub>2</sub>CO, Rh<sub>2</sub>(O<sub>2</sub>CCH<sub>3</sub>)<sub>4</sub>(NIA)<sub>2</sub>·2(CH<sub>3</sub>)<sub>2</sub>CO (**2**)·2(CH<sub>3</sub>)<sub>2</sub>CO and *cis*-Re<sub>2</sub>(O<sub>2</sub>CCH<sub>3</sub>)<sub>2</sub>Cl<sub>4</sub>(INA)<sub>2</sub> (**3**)

	<b>1</b> ·2(CH <sub>3</sub> ) <sub>2</sub> CO	<b>2</b> ·2(CH <sub>3</sub> ) <sub>2</sub> CO	<b>3</b>
Formula	C <sub>26</sub> H <sub>36</sub> N <sub>4</sub> O <sub>12</sub> Rh <sub>2</sub>	C <sub>26</sub> H <sub>36</sub> N <sub>4</sub> O <sub>12</sub> Rh <sub>2</sub>	C <sub>16</sub> H <sub>18</sub> Cl <sub>4</sub> N <sub>4</sub> O <sub>6</sub> Re <sub>2</sub>
Formula weight	802.41	802.41	876.56
Space group	<i>P</i> $\bar{1}$	<i>P</i> $\bar{1}$	<i>P</i> 2 <sub>1</sub> / <i>c</i>
<i>a</i> (Å)	7.2021(14)	7.3768(15)	15.2159(10)
<i>b</i> (Å)	8.2240(16)	8.0472(16)	10.4743(7)
<i>c</i> (Å)	13.503(3)	14.366(3)	15.9726(8)
$\alpha$ (°)	91.83(3)	88.67(3)	90.0
$\beta$ (°)	96.26(3)	89.71(3)	111.429(4)
$\gamma$ (°)	96.54(3)	65.78(3)	90.0
<i>V</i> (Å <sup>3</sup> )	789.0(3)	777.5(3)	2369.7(5)
<i>Z</i>	1	1	4
$\rho_{\text{calcd}}$ (g/cm <sup>3</sup> )	1.69	1.71	2.46
$\mu$ (Mo K $\alpha$ ) (cm <sup>-1</sup> )	11.11	11.28	10.84
Temperature (K)	110	110	173
Reflections collected	3099	3778	17406
Independent	2190	2581	5747
Observed [ <i>I</i> > 2 $\sigma$ ( <i>I</i> )]	1763	2094	4212
Number of variables	189	199	307
<i>R</i> <sub>1</sub> <sup>a</sup>	0.064	0.049	0.045
<i>wR</i> <sub>2</sub> <sup>b</sup>	0.155	0.117	0.103
Goodness-of-fit	1.037	0.967	1.027

<sup>a</sup>  $R_1 = \sum ||F_o| - |F_c|| / \sum |F_o|$  with  $F_o^2 > 2\sigma(F_o^2)$ .

<sup>b</sup>  $wR_2 = [\sum w(|F_o|^2 - |F_c|^2)|^2 / \sum |F_o|^2]^{1/2}$ .

## 2.6. X-ray crystallography

Single crystals of compounds **1–3** were harvested directly from slow diffusion reactions. The data collections for **1** and **2** were performed at  $110 \pm 2$  K on a Bruker SMART 1K CCD platform diffractometer equipped with graphite monochromated Mo  $K\alpha$  radiation ( $\lambda = 0.71069$  Å). The frames were integrated in the Bruker SAINT software package [9], and the data were corrected for absorption using the SADABS program [10]. The structures were solved and refined using the suite of programs in the SHELXTL V.5.10 package [11]. The single crystal X-ray study on complex **3** was carried out on a Nonius Kappa CCD diffractometer. Routine experimental details of the data collection and refinement procedures used to determine the structure of **3** are reported elsewhere [6]. Pertinent crystallographic data for  $\text{Rh}_2(\text{O}_2\text{CCH}_3)_4(\text{INA})_2 \cdot 2(\text{CH}_3)_2\text{CO}$  (**1**)  $\cdot 2(\text{CH}_3)_2\text{CO}$ ,  $\text{Rh}_2(\text{O}_2\text{CCH}_3)_4(\text{NIA})_2 \cdot 2(\text{CH}_3)_2\text{CO}$  (**2**)  $\cdot 2(\text{CH}_3)_2\text{CO}$  and *cis*- $\text{Re}_2(\text{O}_2\text{CCH}_3)_2\text{Cl}_4(\text{INA})_2$  (**3**) are summarized in Table 1.

Two molecules of acetone were located in the interstices of crystals of **1** and **2**. All non-hydrogen atoms in complexes **1–3**, except the atoms N(2) and C(3) of complex **1**, were refined anisotropically. Hydrogen atoms were included in the final stages of the refinement as riding atoms at calculated positions for complexes **1** and **2**. The amide hydrogens (CONH<sub>2</sub>) of complex **3** were located from a difference map and refined isotropically. Remaining hydrogens were placed at calculated positions with  $U(\text{H}) = 1.3 U_{\text{eq}}(\text{C})$ . The highest peaks remaining in the final difference Fourier map of complexes **1–3** are 2.04, 1.67 and 2.40 e Å<sup>-3</sup>, respectively, and are located in the vicinity of the metal atoms.

## 3. Results and discussion

Slow diffusion of isonicotinamide into an acetone solution of  $\text{Rh}_2(\text{O}_2\text{CCH}_3)_4$  results in the formation of purple crystals of (**1**)  $\cdot 2(\text{CH}_3)_2\text{CO}$ . Identical products were obtained while varying the amount of isonicotinamide from equimolar to a significant molar excess as compared to the metal complex concentration. An X-ray structural analysis revealed that, as expected, the compound contains two isonicotinamide ligands in the axial positions of  $\text{Rh}_2(\text{O}_2\text{CCH}_3)_4$  (Fig. 1). Selected distances and angles are listed in Table 2. The Rh–Rh distance of 2.403(2) Å is typical of singly bonded  $\text{Rh}_2^{4+}$  units with axial nitrogen donor ligands [5]. The axial Rh–N distance is 2.205(7) Å and the Rh(1A)–Rh(1)–N(1) angle is 178.1(2)°. The most interesting feature of the crystal structure is the intermolecular, self-complementary hydrogen bonding of the amide groups. Adjacent amide moieties form two head-to-head hydrogen

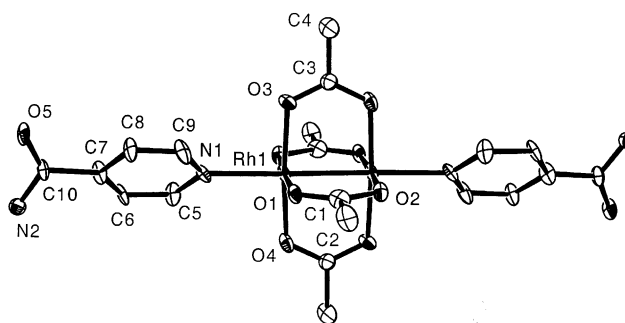


Fig. 1. Thermal ellipsoid plot of  $\text{Rh}_2(\text{O}_2\text{CCH}_3)_4(\text{INA})_2$  in (**1**)  $\cdot 2(\text{CH}_3)_2\text{CO}$  represented at the 50% probability level. Hydrogen atoms have been omitted for the sake of clarity.

Table 2  
Selected bond distances (Å) and bond angles (°) in  $\text{Rh}_2(\text{O}_2\text{CCH}_3)_4(\text{INA})_2 \cdot 2(\text{CH}_3)_2\text{CO}$  (**1**)  $\cdot 2(\text{CH}_3)_2\text{CO}$

<i>Bond distances</i>			
Rh(1)–Rh(1A)	2.4034(16)	Rh(1)–O(4)	2.033(6)
Rh(1)–O(1)	2.036(6)	Rh(1)–N(1)	2.205(7)
Rh(1)–O(2A)	2.028(6)	C(10)–N(2)	1.331(12)
Rh(1)–O(3)	2.044(6)	C(10)–O(5)	1.237(11)
<i>Bond angles</i>			
O(1)–Rh(1)–O(3)	90.6(2)	N(1)–Rh(1)–O(1)	91.0(3)
O(1)–Rh(1)–O(4)	90.2(2)	N(1)–Rh(1)–Rh(1A)	178.1(2)
O(1)–Rh(1)–O(2A)	176.3(2)	N(2)–C(10)–O(5)	124.4(8)

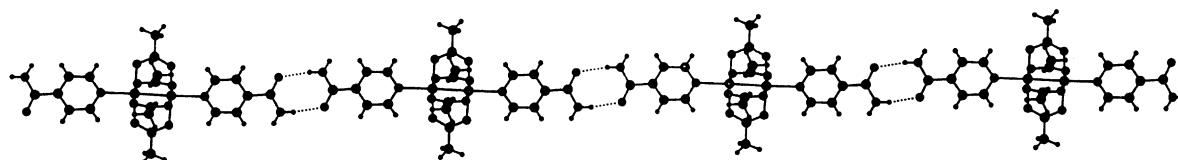


Fig. 2. Hydrogen-bonded infinite linear network of  $\text{Rh}_2(\text{O}_2\text{CCH}_3)_4(\text{INA})_2$ .

bonds of the type  $\text{N}-\text{H}\cdots\text{O}$  ( $\text{N}(2)\cdots\text{O}(5) = 2.922(10) \text{ \AA}$ ), the result of which is the formation of a linear chain of  $\text{Rh}_2(\text{O}_2\text{CCH}_3)_4(\text{INA})_2$  molecules supported by hydrogen bonds. The linear propagation of the dirhodium vector through the isonicotinamide ligands in the crystal structure is shown in Fig. 2.

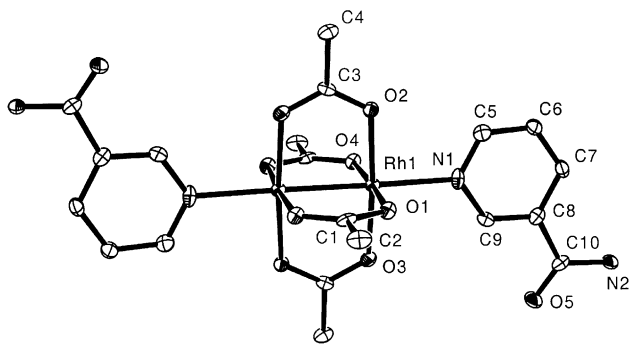


Fig. 3. Thermal ellipsoid plot of  $\text{Rh}_2(\text{O}_2\text{CCH}_3)_4(\text{NIA})_2$  in  $(2) \cdot 2(\text{CH}_3)_2\text{CO}$  represented at the 50% probability level. Hydrogen atoms have been omitted for the sake of clarity.

The molecular structure of  $\text{Rh}_2(\text{O}_2\text{CCH}_3)_4(\text{NIA})_2 \cdot 2(\text{CH}_3)_2\text{CO}$  is very similar to that of  $(1) \cdot 2(\text{CH}_3)_2\text{CO}$ . Two nicotinamide ligands are bound to the axial positions at the pyridine sites, and intermolecular amide–amide hydrogen bonding interactions are evident ( $\text{N}(2)\cdots\text{O}(5) = 2.865(7) \text{ \AA}$ ). A thermal ellipsoid plot of the molecular building blocks is provided in Fig. 3, and selected distances and angles are listed in Table 3. The orientation of the hydrogen bonds involving the nicotinamide ligands is *anti* in this structure which leads to a zig-zag motif (Fig. 4).

The axial water ligands in the quadruply bonded complex  $\text{cis-Re}_2(\text{O}_2\text{CCH}_3)_2\text{Cl}_4(\text{H}_2\text{O})_2$  are readily replaced by isonicotinamide ligands to yield the crystalline compound  $\text{cis-Re}_2(\text{O}_2\text{CCH}_3)_2\text{Cl}_4(\text{INA})_2$  (**3**). A thermal ellipsoid plot of the molecules is shown in Fig. 5, and selected distances and angles are provided in Table 4. The  $\text{Re}(1)-\text{Re}(2)$  distance of  $2.2493(4) \text{ \AA}$  is characteristic of a Re–Re quadruple bond, and is slightly longer than the Re–Re bond of  $2.224(5) \text{ \AA}$  in  $\text{cis-Re}_2(\text{O}_2\text{CCH}_3)_2\text{Cl}_4(\text{H}_2\text{O})_2$ . The Re–O and Re–Cl distances are typical of

Table 3

Selected bond distances ( $\text{\AA}$ ) and bond angles ( $^\circ$ ) in  $\text{Rh}_2(\text{O}_2\text{CCH}_3)_4(\text{NIA})_2 \cdot 2(\text{CH}_3)_2\text{CO}$

Bond distances			
Rh(1)–Rh(1A)	2.3972(12)	Rh(1)–O(4)	2.040(4)
Rh(1)–O(1)	2.047(4)	Rh(1)–N(1)	2.224(5)
Rh(1)–O(2)	2.030(4)	C(10)–N(2)	1.326(9)
Rh(1)–O(3)	2.035(4)	C(10)–O(5)	1.226(8)
Bond angles			
O(1)–Rh(1)–O(2)	89.31(16)	N(1)–Rh(1)–O(1)	93.15(18)
O(1)–Rh(1)–O(3)	90.26(17)	N(1)–Rh(1)–Rh(1A)	178.36(14)
O(1)–Rh(1)–O(4)	176.01(16)	N(2)–C(10)–O(5)	122.8(6)

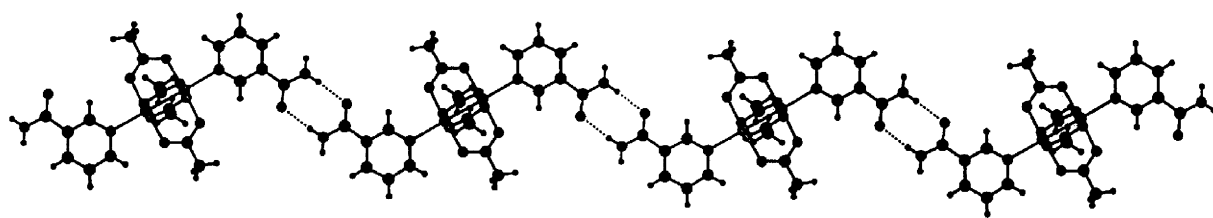


Fig. 4. Hydrogen-bonded zig-zag motif of the infinite network of  $\text{Rh}_2(\text{O}_2\text{CCH}_3)_4(\text{INA})_2$ .

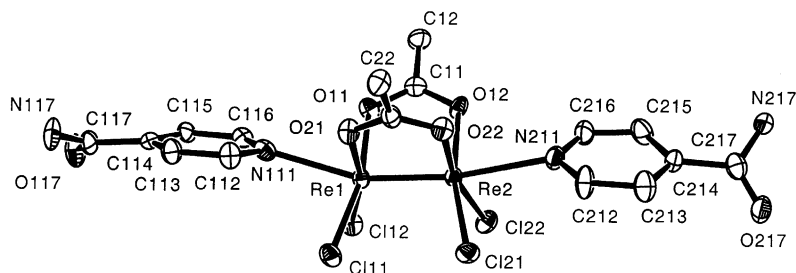


Fig. 5. Thermal ellipsoid plot of  $\text{cis-Re}_2(\text{O}_2\text{CCH}_3)_2\text{Cl}_4(\text{INA})_2$  (**3**) represented at the 50% probability level. Hydrogen atoms have been omitted for the sake of clarity.

Table 4  
Selected bond distances (Å) and bond angles (°) in  $[cis-Re_2(O_2CCH_3)_2Cl_4(INA)_2]$  (3)

Bond distances			
Re(1)–Re(2)	2.2493(4)	Re(2)–N(211)	2.509(7)
Re(1)–O(11)	2.050(6)	C(117)–N(117)	1.332(13)
Re(1)–O(21)	2.044(6)	C(117)–O(117)	1.238(12)
Re(1)–Cl(11)	2.309(2)	C(217)–N(217)	1.351(13)
Re(1)–Cl(12)	2.327(2)	C(217)–O(217)	1.232(12)
Re(1)–N(111)	2.420(8)		
Bond angles			
O(21)–Re(1)–O(11)	88.9(2)	Cl(21)–Re(2)–Cl(22)	91.54(8)
Cl(11)–Re(1)–Cl(12)	89.58(8)	Re(1)–Re(2)–N(211)	169.64(17)
Re(2)–Re(1)–N(111)	161.21(17)	O(117)–C(117)–N(117)	122.5(9)
O(12)–Re(2)–O(22)	89.2(2)	O(217)–C(217)–N(217)	121.6(9)

the values reported for similar complexes [12], and the Re–Re–O angles are close to 90° (they range from 88.7(2)° to 90.6(2)°). The corresponding angles involving the equatorial Cl<sup>−</sup> ligands are much wider (range 101.8(1)°–105.2(1)°). This ‘bending back’ of the chloride ligands away from the Re–Re bond and towards the axial sites leads to a marked non-linearity of the Re–Re–N (axial) units as evidenced by the Re(1)–Re(2)–N(211)

and Re(2)–Re(1)–N(111) angles of 161.2(2)° and 169.6(2)°.

In a manner akin to the situation in  $Rh_2(O_2CCH_3)_4(INA)_2 \cdot 2(CH_3)_2CO$ , the adjacent amide–amide hydrogen bonds ( $N(117) \cdots O(217) = 2.913(10)$  Å and  $N(217) \cdots O(117) = 2.963(10)$  Å) serve to stitch the individual  $cis-Re_2(O_2CCH_3)_2Cl_4(INA)_2$  molecules into an infinite chain (Fig. 6). The self-complementary hydrogen

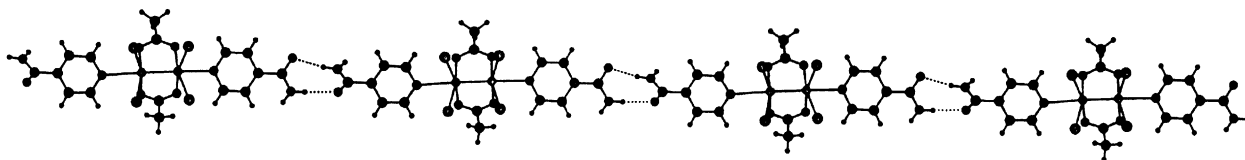


Fig. 6. Hydrogen-bonded linear infinite network of  $cis-Re_2(O_2CCH_3)_2Cl_4(INA)_2$ .

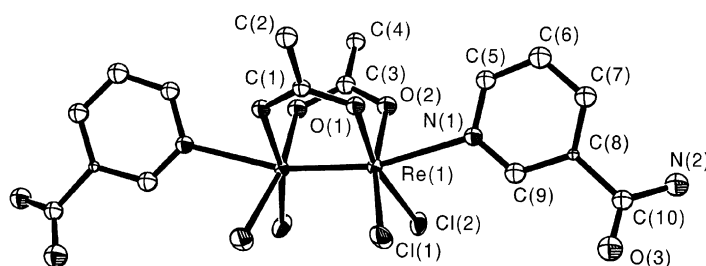


Fig. 7. Thermal ellipsoid plot of  $cis-Re_2(O_2CCH_3)_2Cl_4(NIA)_2$  in  $4 \cdot 2(NIA)$  represented at the 50% probability level. Hydrogen atoms have been omitted for the sake of clarity.

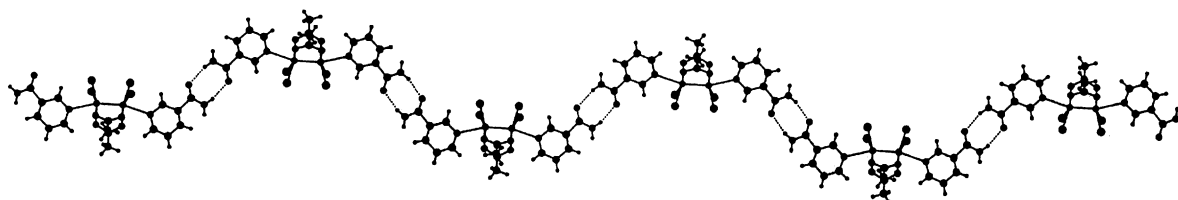


Fig. 8. Hydrogen-bonded sinusoidal pattern of the infinite network of  $cis-Re_2(O_2CCH_3)_2Cl_4(NIA)_2$ .

bonding ability of the amide group, situated at the 4 position of the pyridine ring of the isonicotinamide ligand, governs the singular main feature of the crystal structure, namely the formation of a 1-D linear polymeric network.

The reaction of *cis*-Re<sub>2</sub>(O<sub>2</sub>CCH<sub>3</sub>)<sub>2</sub>Cl<sub>4</sub>(H<sub>2</sub>O)<sub>2</sub> with nicotinamide produces the compound *cis*-Re<sub>2</sub>(O<sub>2</sub>CCH<sub>3</sub>)<sub>2</sub>Cl<sub>4</sub>(NIA)<sub>2</sub>·2(NIA) (**4**)·2(NIA), as determined by elemental analysis and a preliminary crystal structure determination [13]. Unlike the other three structures, this compound crystallizes with two molecules of nicotinamide in the interstices. Although the data did not refine as well as the other three structures, it was possible to locate all of the atoms in the difference Fourier map. A thermal ellipsoid plot of the molecules is shown in Fig. 7. As expected, the amide groups at the 3 position of the pyridine ring are engaged in head-to-head hydrogen bonding interactions, but unlike complex **2**, the *syn* disposition of the NIA ligands on each dirhenium building unit leads to hydrogen bonds that form a sinusoidal pattern (Fig. 8).

#### 4. Conclusion

Four dirhodium and dirhenium complexes with isonicotinamide and nicotinamide ligands have been prepared and shown to consist of individual M<sub>2</sub> building blocks that form a polymeric network in the solid state as a result of self-complementary hydrogen bonds. The major features of the crystal structures of these complexes are dictated by the well-defined characteristics of the supramolecular interactions. The use of the isonicotinamide ligands results in the formation of linear structures, while the nicotinamide ligands form structures with a zig-zag or sinusoidal pattern. Our results indicate that these sets of ligands offer a tool to organize electron rich dimetal centers into arrays which are useful for promoting interesting properties.

#### Acknowledgements

We thank Dr. Phillip E. Fanwick for his help in collecting the diffraction data of complex **3**. K.R.D. gratefully acknowledges the Welch Foundation and the National Science Foundation for a PI Grant (CHE-9906583) and for equipment grants to purchase the CCD X-ray equipment (CHE-9807975). K.R.D. also thanks Johnson-Matthey for a generous loan of rhodium trichloride. T.-T.V. would like to thank the NASA SHARP high-school program for the opportunity to work in a research laboratory.

#### References

- [1] (a) See, for example: M. Fujita, Chem. Soc. Rev. 27 (1998) 417; (b) S. Leininger, B. Olenyuk, P.J. Stang, Chem. Rev. 100 (2000) 853; (c) B.J. Holliday, C.A. Mirkin, Angew. Chem., Int. Ed. 40 (2001) 2022, and references therein.
- [2] (a) M. Munakata, L.P. Wu, M. Yamamoto, T. Kuroda-Sowa, M. Maekawa, J. Am. Chem. Soc. 118 (1996) 3117; (b) M. Scudder, I. Dance, J. Chem. Soc., Dalton Trans. (1998) 3167; (c) J.C.M. Rivas, L. Brammer, New J. Chem. 22 (1998) 1315; (d) C.-W. Chan, D.M.P. Mingos, D.J. Williams, J. Chem. Soc., Dalton Trans. (1995) 2469; (e) A.S. Batasanov, P. Hubberstey, C.E. Russel, P.H. Walton, J. Chem. Soc., Dalton Trans. (1997) 2667.
- [3] (a) C.J. Kuehl, F.M. Tabellion, A.M. Arif, P.J. Stang, Organometallics 20 (2001) 1956; (b) D. Braga, L. Maini, F. Grepioni, C. Elschenbroich, F. Paganelli, O. Schiemann, Organometallics 20 (2001) 1875; (c) C.B. Aakeröy, A.M. Beatty, D.S. Leinen, K.R. Lorimer, Chem. Commun. (2000) 935; (d) C.B. Aakeröy, A.M. Beatty, D.S. Leinen, J. Am. Chem. Soc. 120 (1998) 7383; (e) C.B. Aakeröy, A.M. Beatty, D.S. Leinen, Angew. Chem., Int. Ed. 38 (1999) 1815; (f) C.B. Aakeröy, A.M. Beatty, Chem. Commun. (1998) 1067.
- [4] (a) F.A. Cotton, C. Lin, C.A. Murillo, Acc. Chem. Res. 34 (2001) 759, and references therein; (b) J.K. Bera, B.W. Smucker, R.A. Walton, K.R. Dunbar, Chem. Commun. (2001) 2562; (c) J.K. Bera, P. Angaridis, F.A. Cotton, M.A. Petrukhina, P.E. Fanwick, R.A. Walton, J. Am. Chem. Soc. 123 (2001) 1515; (d) R.H. Cayton, M.H. Chisholm, J.C. Huffman, E.B. Lobkovsky, J. Am. Chem. Soc. 113 (1991) 8709.
- [5] F.A. Cotton, E.V. Dikarev, M.A. Petrukhina, M. Schmitz, P.J. Stang, Inorg. Chem. 41 (2002) 2903, and references therein.
- [6] Y. Ding, S.S. Lau, P.E. Fanwick, R.A. Walton, Inorg. Chim. Acta 300–302 (2000) 505.
- [7] A.R. Chakravarty, F.A. Cotton, A.R. Cutler, R.A. Walton, Inorg. Chem. 25 (1986) 3619.
- [8] G.A. Rempel, P. Legzdins, H. Smith, G. Wilkinson, Inorg. Synth. 13 (1972) 87.
- [9] SAINT, Program for area detector absorption correction, Siemens Analytical X-Ray Instruments Inc., Madison, WI 53719, 1994–1996.
- [10] G.M. Sheldrick, SADABS, Program for Siemens Area Detector Absorption Correction, Univ. of Göttingen, Germany, 1996.
- [11] SHELXTL version 5.10, Reference Manual, Bruker Industrial Automation, Analytical Instrument, Madison, WI 53719, 1999.
- [12] F.A. Cotton, R.A. Walton, Multiple Bonds Between Metal Atoms, second ed., Clarendon Press, Oxford, 1993.
- [13] Preliminary crystallographic data for complex (**4**)·2(NIA): C<sub>28</sub>H<sub>30</sub>Cl<sub>4</sub>N<sub>8</sub>O<sub>8</sub>Re<sub>2</sub>, *M* = 1120.80, Orthorhombic, *Pnma*, *a* = 12.817(3), *b* = 33.145(7), *c* = 8.3812(17) Å, *V* = 3560.6(12) Å<sup>3</sup>, *Z* = 4, *T* = 110 ± 2 K, *D*<sub>c</sub> = 2.10 g cm<sup>-3</sup>, μ(Mo Kα) = 7.15 cm<sup>-1</sup>, reflections collected/independent/observed 17252/3008/2216, *R*<sub>int</sub> (*R*<sub>σ</sub>) = 0.0694(0.0712), *R* = 0.0862, GoF = 1.149. Bond distances (Å): Re(1)–Re(2) 2.2479(14), Re(1)–O(1) 1.966(5), Re(1)–O(2) 2.035(12), Re(1)–Cl(1) 2.289(5), Re(1)–Cl(2) 2.294(5), Re(1)–N(1) 2.462(15). Angles (°): Re(2)–Re(1)–N(1) 164.4(4), O(1)–Re(1)–O(2) 88.6(5), O(1)–Re(1)–Cl(1) 87.9(4), Re(2)–Re(1)–Cl(2) 104.60(13).